Journal of Applied Electrochemistry (2020) 50:431–438
https://doi.org/10.1007/s10800-020-01401-8

RESEARCH ARTICLE

Enhancement of the lithium titanium oxide anode performance by the copolymerization of conductive polypyrrole with poly(acrylonitrile/butyl acrylate) binder

Yanchunxiao Qi[1] · Minh Hien Thi Nguyen[1] · Eun-Suok Oh[1]

Received: 13 August 2019 / Accepted: 3 February 2020 / Published online: 21 February 2020

Abstract
An eco-friendly conductive water-dispersed polymer binder was used in lithium-ion batteries (LIBs) for the first time. A conductive polypyrrole (PPy) was copolymerized successfully into an adhesive poly(acrylonitrile/butyl acrylate) (PANBA) emulsified binder to impart two important properties to the PANBA-PPy binder system simultaneously: adhesion and electronic conduction. These two properties ultimately help the active materials of the LIB to exert better electrochemical performance. The copolymers were synthesized via two-step polymerization with different weights of pyrrole monomer. With the incorporation of PPy, the electrical resistance of the copolymer was reduced significantly, and the increase in PPy content of the binder system also decreased the resistance. The electrochemical performance of the conductive copolymers as a binder for the $Li_4Ti_5O_{12}$ (LTO) anodes of lithium-ion batteries was superior to the non-conductive PANBA binder. At relatively low charge/discharge current densities, the more conductive PANBA-PPy4 binder was favorable to the cyclic performance of the LTO electrodes, whereas the PANBA-PPy2 sample has prominent high rate performance at a current density of 10 C because of its adhesive properties and conductive characteristics.

✉ Eun-Suok Oh
esoh1@ulsan.ac.kr

[1] School of Chemical Engineering, University of Ulsan, 93 Daehak-ro, Nam-gu, Ulsan 44610, Republic of Korea

Graphic Abstract

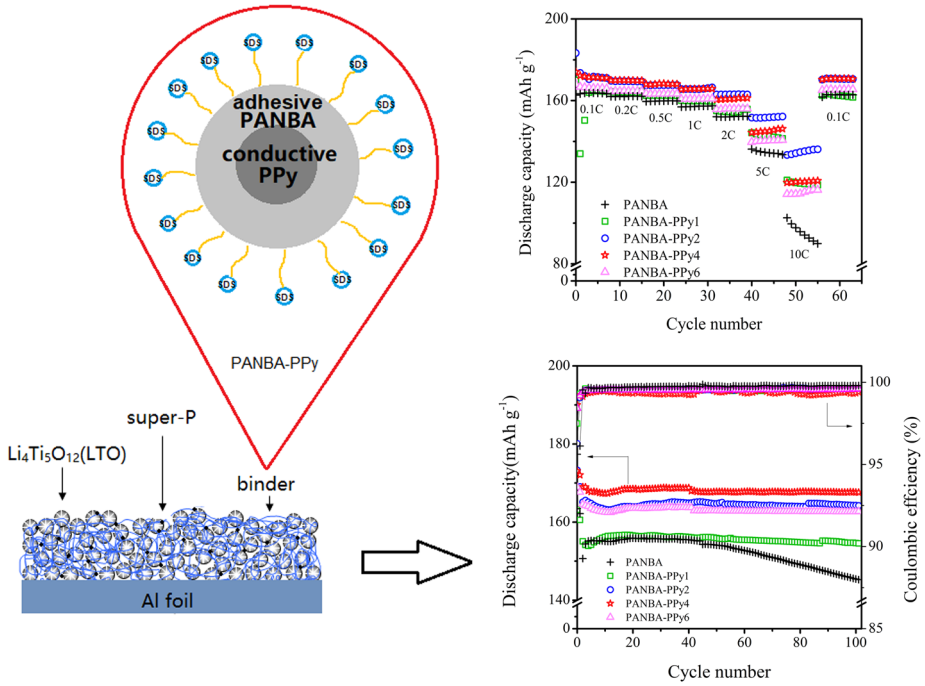

Keywords Polypyrrole · Poly(acrylonitrile/butyl acrylate) · Conductive polymer · Water-dispersed binder · Lithium titanium oxide anode · Lithium-ion battery

1 Introduction

The lithium-ion battery (LIB) is becoming increasingly popular as a power source for portable electronic devices and electric vehicles because of its high energy density [1, 2]. To achieve high battery performance, one of the key factors is to improve the characteristics of the polymer binder. With an effective binder, the components such as the active materials and conducting agents in the composite electrodes can be well connected to the current collector, ultimately leading to good electrochemical performance during the charge and discharge processes [3–5]. In recent years, many studies have assessed several kinds of polymer binder to enhance their adhesion strength, processability, or environmental friendliness, e.g., polyacrylic acid [6–8], polyacrylamide [5, 9], polyrotaxenes [10], and alginate [11, 12].

The electrical conductivity of the binder also plays an important role for better cycling performance [13–18]. Liu et al. [13] reported that a conductive poly(9,9-dioctylfluorene-co-fluorenone-co-methylbenzoic ester) binder could maintain the electrical network of the electrode, even after the huge volumetric expansion/contraction of a silicon electrode, and greatly enhance the electrochemical performance of the high-capacity electrode. The use of a graphene nanofiller in a polyvinylidene fluoride (PVdF) binder was reported to improve significantly the high rate capability of a high-powered lithium titanium oxide (LTO) electrode [14]. Unfortunately, most of these studies were limited to organic-soluble or water-soluble polymer binders. Less effort has been paid to improving the electrical conductivity of water-dispersed polymer binders. Indeed, many commercial LIB industries use water-dispersed polymer binders, such as styrene-butadiene rubber (SBR) with a carboxymethyl cellulose (CMC) thickening agent, because of its excellent adhesion, flexibility, and lack of environmental issues [19–21]. Therefore, few studies have examined ways to enhance the binder performance of water-dispersed polymers. For instance, water-dispersed poly(acrylonitrile-co-butyl acrylate) (PANBA) exhibited superior binder performance for LIB anodes over typical SBR [22, 23]. On the other hand, no studies have been done to improve the electrical conductivity of water-dispersed polymer binders.

Typical electrically conducting polymers (ECPs), such as polyaniline (PANi), polypyrrole (PPy), polyacetylene, and polythiophene (PT), have conjugated bonds so that delocalized pi electrons can move freely through the polymeric chain. Of these, PANi and PTs have often been applied to LIBs as the binder of electrodes [16, 24–29]. Unfortunately, conducting polymers usually have low adhesion and do not maintain the mechanical integrity of the electrodes after

long-term cycling. This is why conducting polymers are normally used in conjunction with highly adhesive polymers, such as carboxymethyl chitosan [28] and polyacrylic acid [29], when applied to a binder. PPy is air stable and easy to prepare by either chemical or electrochemical methods and shows very good electrical properties when used in electrochemical applications [30]. In this study, PPy was introduced to the conductive component of the water-dispersed PANBA binder. The PANBA-PPy binder system was applied to LTO electrodes as an eco-friendly conductive water-dispersed binder, which is the first report of such use. A variety of physical and electrochemical characterization techniques will be employed to examine how the conductive PPy component in a binder affects the electrochemical performance of LTO electrodes.

2 Experimental

2.1 Preparation of poly(acrylonitrile/butyl acrylate)-polypyrrole

PANBA was first synthesized using the emulsion polymerization method described elsewhere [22]. To prepare for PPy polymerization, a small amount of sodium dodecyl sulfate (SDS, Tokyo Chemical Industry Co.) was then added to 115 g of PANBA emulsion containing 30 g PANBA with pyrrole (Alfa Aesar) monomer ranging in weight from 1 to 6 g. Finally, a certain amount of potassium persulfate (KPS, Sigma-Aldrich) corresponding to one part of the pyrrole monomer was introduced to initiate the polymerization of pyrrole. The reaction was carried out at a constant temperature of 70 °C for 2 h before being cooled to room temperature. For convenience, the PANBA-PPy binders are referred to as follows: PANBA-PPy1, PANBA-PPy2, PANBA-PPy4, and PANBA-PPy6, where the number indicates the mass of PPy (in grams) in the binder. Thus, PPy contents in the copolymers are 3.23% in PANBA-PPy1, 6.25% in PANBA-PPy2, 11.8% in PANBA-PPy4, and 16.7% in PANBA-PPy6, respectively.

2.2 Preparation of the LTO electrodes and coin-half cells

LTO electrodes were prepared with 90 wt% LTO active material, 5 wt% conductive super-P, 2 wt% high-viscosity CMC (Daicel FineChem Ltd., Japan), and 3 wt% PANBA-PPy binders based on the solid contents. All the materials were mixed using a homogenizer (Nissei ACE AM-2, Japan) for 45 min. For comparison, PANBA was also used as a binder for the LTO electrode. The mixed slurry was casted onto a 20-μm-thick Al foil. After drying in a convection oven at 60 °C for 30 min, the electrodes were roll pressed and placed in a vacuum oven maintained at 70 °C for 1 day before being assembled into CR2032-type coin-half cells in an argon-filled glove box. A solution of 1M $LiPF_6$ in 1:1:1 ethylene carbonate: dimethyl carbonate: ethyl methyl carbonate by volume (Panaxetec Co., Korea) and lithium metal were used as the electrolyte and counter electrode, respectively.

2.3 Physical and electrochemical characterization of binders and electrodes

The electrical resistance of the PANBA-PPy films was measured using a 4-point probe (CMT-100MP, Advanced Instrument Technology). Thin binder films after being dried in a convection oven at 40 °C overnight were cut to 14-mm-diameter coins and their sheet resistances were measured. The polymers were analyzed by Fourier-transform infrared (FT-IR, Thermo Scientific Nicolet iS5) spectroscopy over the wavenumber range, 500–3900 cm^{-1}. Thermogravimetric analysis (TGA, Q50 TA Instrument) of the binder polymers was carried out under a nitrogen atmosphere at a temperature range from room temperature to 750 °C at a heating rate of 10 °C min^{-1}. To assess the wettability of the binder films, an optical tensiometer (Theta Lite, Biolin Scientific) was used to record the contact angle of an electrolyte droplet placed on each PANBA-PPy film for 1 min.

Transmission electron microscopy (TEM, JEM-2100F, JEOL, Japan) was used to examine the morphology of the PANBA-PPy copolymer. To measure the adhesion strength between the LTO electrode and Al current collector as well as among the electrode components, 2-cm-wide electrode strips were peeled at 180° using a texture analyzer (TA-Plus, Lloyd Instruments Ltd.) at a propagation speed of 60 mm min^{-1}. The electrochemical performance was characterized within the voltage range of 1.0 V to 2.6 V using a battery cycler (WBCS3000, Wonatech, Korea). For the cycling performance, the coin cells were charged/discharged at 0.1 C for the first two cycles and at 1 C for the subsequent 100 cycles. Rate capability tests of the cells were also performed in a variety of charge/discharge currents ranging from 0.1 to 10 C. Electrochemical impedance spectroscopy (EIS, VSP, BioLogic Science Instruments) was conducted over the frequency range, 100 kHz to 0.01 Hz.

3 Results and discussion

A water-dispersed emulsion is normally stored at most for 6 months before being applied to LIBs as a polymer binder. Therefore, the emulsion stability must be checked. In this study, the stability of the PANBA-PPy emulsion was examined using a Turbiscan aging station (Turbiscan LAB, Formulaction Co., France) by scanning the samples at 30 °C

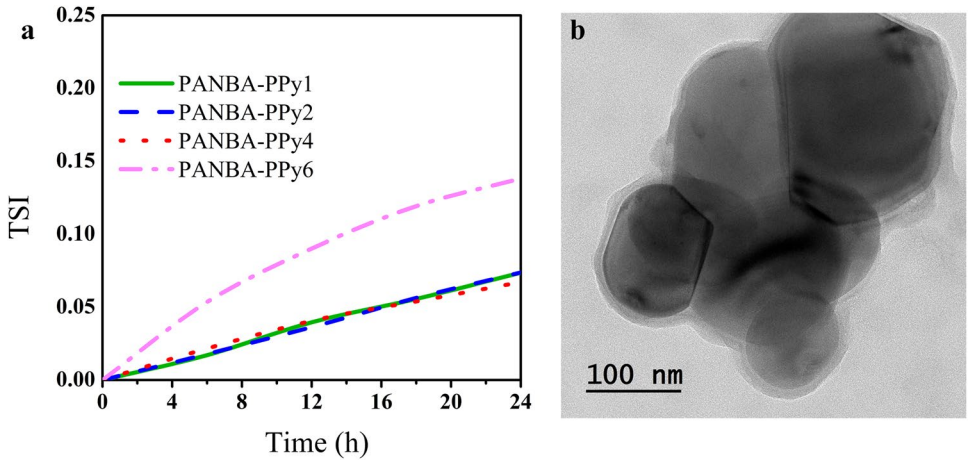

Fig. 1 **a** Turbiscan stability index of the PANBA-PPy samples measured over a 24 h period. **b** High-resolution TEM image of the PANBA-PPy2 sample

for 24 h. The Turbiscan analysis technique describes the sample destabilization, such as creaming, sedimentation, flocculation, aggregation, and coalescence, according to the backscattering and transmission signals, and represents the destabilization as a value of the Turbiscan Stability Index (TSI). Higher TSI values mean that more destabilization occurred in the sample. Figure 1a presents the TSI of the PANBA-PPy emulsion samples over a 24 h period. The PANBA-PPy6 emulsion containing a relatively large amount of PPy (6 g) showed a much higher TSI compared to the other samples. This explains why a sample exceeding 6 g PPy could be synthesized, despite the potential increase in electrical conductivity with increasing PPy content. In addition to TSI, the morphology of the PANBA-PPy2 sample, as an example, was observed by TEM, as shown in Fig. 1b. The sample was coated on a copper grid and dried before being characterized. Owing to the two-step emulsion polymerization, an approximately 10-nm-thick thin outer shell, probably corresponding to PPy, encompasses the inner PANBA core. This morphology is similar to that of the PPy/poly(styrene sulfonate) composite reported elsewhere [31]. Although a few particles aggregated, as shown in the figure, the PANBA-PPy2 sample was much more stable than the PPy sample. In addition to the TEM result, the FT-IR spectra of PPy, PANBA, and PANBA-PPy2 binder films in Fig. 2 indicate a successful copolymerization of PPy to PANBA. The spectrum of PANBA-PPy2 reveals the characteristic peaks at 1545 cm^{-1} (C=N), 1731 cm^{-1} (C=O), and 2241 cm^{-1} (C≡N) which are attributed to the fundamental vibrations of PPy ring, the stretching vibration of carbonyl in butyl acrylate, and the stretching vibration of nitrile groups in acrylonitrile, respectively [32–34].

As mentioned previously, the main objective to incorporate PPy in PANBA is to improve the electrical conductivity of the binder system, ultimately leading to significant improvements in the electrochemical performance of the LTO electrodes. The improvement in the electrical

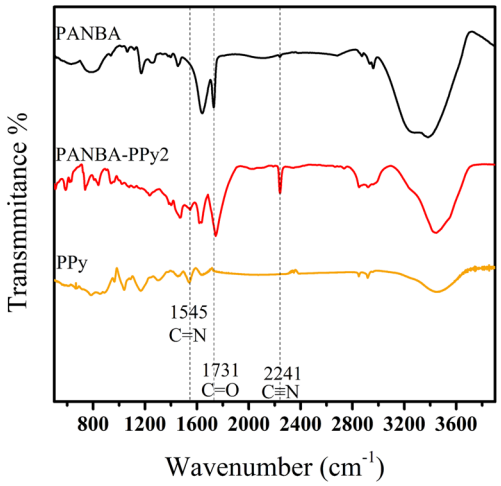

Fig. 2 FT-IR spectra of PPy, PANBA, and PANBA-PPy2 binder films

Table 1 Sheet resistance of the PANBA-PPy samples containing different amounts of polypyrrole.

	PANBA-PPy1	PANBA-PPy2	PANBA-PPy4	PANBA-PPy6	PANBA
R(Ω sq^{-1})	133.8	114.7	91.3	72.3	Out of range

conductivity of the PANBAs copolymerized with different amounts of PPy is highlighted by the sheet resistance of the thin PANBA-PPy films, which are listed in Table 1. As expected, the presence of PPy in the copolymer reduced the sheet resistance of the PANBA to a measurable value from out of the range of the 4-point probe station, and an increase in the PPy content decreased the sheet resistance significantly. This produced a better electron transfer pathway in the LTO electrode.

Electrodes are generally exposed to temperatures higher than 100 °C during the drying process and to extremely

high temperatures under thermal runaway initiated for several reasons, such as overcharge, solid electrolyte interface breakdown, and undesirable electrolyte reactions with lithium ions. In such harsh situations, decomposition of the polymer binder at low temperatures worsens the situation, making it uncontrollable. Unfortunately, the synthesized PPy begins to decompose at relatively low temperatures (< 200 °C) compared to typical polymers, as shown in Fig. 3. This is one of the reasons why the sole use of PPy is not applicable to the binder of LIBs, regardless of its low adhesion capability. On the other hand, all of the PANBA-PPy samples decomposed at temperatures higher than 350 °C and an increase in the PPy content reduced the thermal stability of the samples slightly. In addition, the PANBA-PPy6 sample showed clear weight loss caused by the decomposition of PPy, even though the loss was much smaller than that caused by the decomposition of random PANBA blocks in the PANBA-PPy.

To check the wettability of the PANBA-PPy binder over the electrolyte, the contact angle of an electrolyte droplet placed on the binder film was measured as a function of time; the results are shown in Fig. 4a. The contact angle provides information on the affinity between the polymer binder and the electrolyte. A lower contact angle generally indicates higher affinity between the polymer and electrolyte and implies a favorable circumstance for the transport of lithium ions in the electrolyte through the binder film. As shown in Fig. 4a, after placing an electrolyte droplet onto the binder film, the contact angles of all the samples were quite stable for 60 s. The increase in PPy content reduced the contact angle considerably from 75° for PANBA to approximately 30° for 4 or 6 g of PPy-containing PANBA-PPy. This might be due to the hydrogen bonding between the NH groups in the PPy and the carbonyl groups in the carbonates of the electrolyte. Geiβler et al. [35] suggested that a hydrogen bond arises from the interactions between the carbonyl groups in the insulating poly(bisphenol-A-carbonate) polymer and NH groups in the PPy. In addition to hydrogen bonding, the use of an extra SDS surfactant during PPy polymerization might also contribute to the lower contact angle by decreasing the surface tension.

The adhesion strength of the LTO electrodes containing different PANBA-PPy binders was examined, even though the adhesion property of the LTO is not as important as that for graphite or silicon electrodes experiencing relatively large volume changes during cycling [36]. The LTO electrode has almost zero strain during use so that its electrochemical cycling performance is quite stable for lengthy cycling durations without mechanical damage, such as cracks and delamination. Nevertheless, critical adhesion for manufacturing the electrode and enduring the high current cycles is required for the LTO electrodes. Figure 4b presents the adhesion strength of the LTO electrodes measured through 180° peel tests. As expected from the lower contribution of PPy to the adhesion and its morphology shown in Fig. 1b, an increase in the amount of PPy in the binder content decreases the adhesion of the LTO electrodes gradually.

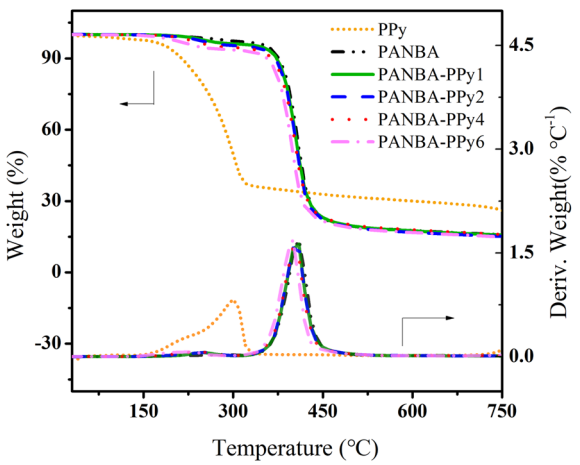

Fig. 3 TGA results of the PANBA-PPy samples and PPy

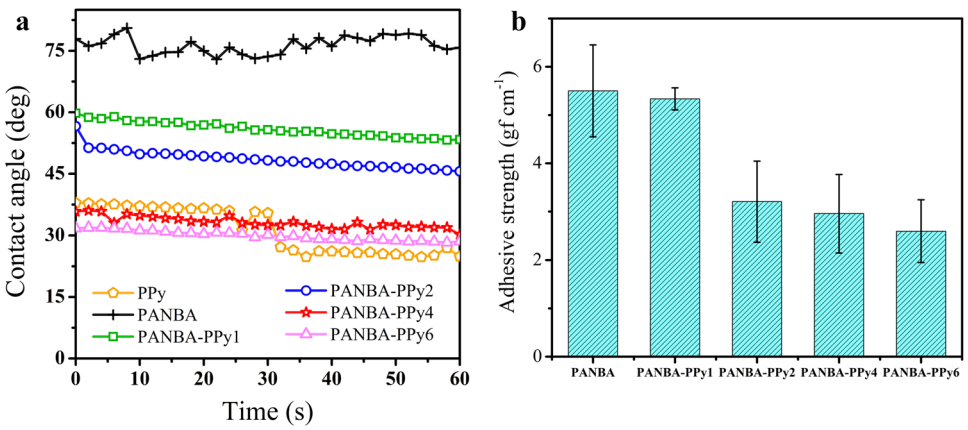

Fig. 4 **a** Contact angle of an electrolyte droplet placed on the binder films as a function of time. **b** 180° peel strength of the LTO electrodes containing different PANBA-PPy samples as a binder

The cycling performance of the LTO electrodes using the synthesized binders was characterized, as shown in Fig. 5a. Compared to previous studies [36, 37], the initial coulombic efficiency of 95.6% for the non-conductive PANBA-containing electrode was higher, and the results were much better for the conductive PANBA-PPy samples, up to 98.6%. In addition, all the LTO electrodes containing the PANBA-PPy samples showed very stable capacities for 100 cycles at 1 C with capacity retention in the range of 94.7–96.8%. The PANBA-PPy4 sample showed the highest cycling capacity of 162.62 mAh g^{-1} at the 100th cycle, which is close to the theoretical capacity of 175 mAh g^{-1}. In contrast, the PANBA-containing LTO electrode retained only 88.9% of its original capacity. This can be explained by the higher electrical conductivity (see Table 1) and better electrolyte wettability (see Fig. 4a) of the PPy-containing binders, providing more effective ways for electron and ion transfer, respectively. These led to relatively small capacity loss in PANBA-PPy2, PANBA-PPy4, and PANBA-PPy6 electrodes compared to the PANBA-PPy1 and PANBA electrodes. This helps confirm the effect of PPy conducting moiety in the PANBA-PPy binders on enhancing the electrochemical performance of the LTO electrodes'.

Figure 5b shows the EIS results of the five-cycled LTO electrodes. The charge transfer resistance of the electrodes was determined from the size of the semicircles at the middle frequency range. These were 22.58 Ω, 19.23 Ω, 17.47 Ω, 14.29 Ω, and 17.93 Ω for the PANBA, PANBA-PPy1, PANBA-PPy2, PANBA-PPy4, and PANBA-PPy6-containing electrodes, respectively. The LTO electrodes containing the PPy component in the binder have lower charge transfer resistance than those composed of the PANBA binder only. In particular, the PANBA-PPy4-containing LTO electrode has the least charge transfer resistance. Obviously, the improvement in the electrical conductivity and ion transportation helps reduce the charge transfer resistance for the electrochemical reactions. On the other hand, the LTO electrode containing PANBA-PPy6 showed relatively larger charge transfer resistance than that of the PANBA-PPy4 sample. This may be due to the loose electrode contact to the current collector caused by the relatively low adhesion of the PANBA-PPy6 sample, as shown in Fig. 4b. Nevertheless, the impedance result is in accordance with the cycling performance result.

Separately, the effects of the conductive PANBA-PPy binders on the rate capability of the LTO electrodes were investigated, as shown in Fig. 6. As expected, the LTO electrodes using the conductive PANBA-PPy binders exhibited much better performance than the non-conductive PANBA binder for any current density. In particular, the difference in performance between the conductive and non-conductive binders was slightly clearer at relatively large current densities. Of the conductive binder, the PANBA-PPy2 samples showed the best rate capability with high cycling capacity. To observe the difference clearly, Fig. 6b shows the percentage of average capacity at a certain current density compared to the average capacity at 0.1 C. At relatively low current densities (< 1 C), there was little difference among PANBA-PPy1, PANBA-PPy2, and PANBA-PPy4. They maintained greater than 95% capacity at 1 C, compared to that at 0.1 C. The difference became greater as the current density was increased. At the highest charge/discharge currents of 10 C, the PANBA-PPy2-containing LTO electrode was found to be superior to any other conductive PANBA-PPy binders. This was attributed to the mechanical strength of the electrodes. The electrode can be damaged easily at such a large current, so that it is favorable to have high mechanical strength imparted by the adhesion. This is why the PANBA-PPy2 sample exhibited better rate capability than the PANBA-PPy4 sample, which has the best cycling performance, as shown in Fig. 5, even though the electronic and ionic transport of PANBA-PPy2 were inferior to those of PANBA-PPy4. The electrodes recovered their capacities up to 93% when they were returned to 0.1 C from 10 C current rates.

Overall, low electronically conductive LTO materials are affected strongly by the conductivity of the binder

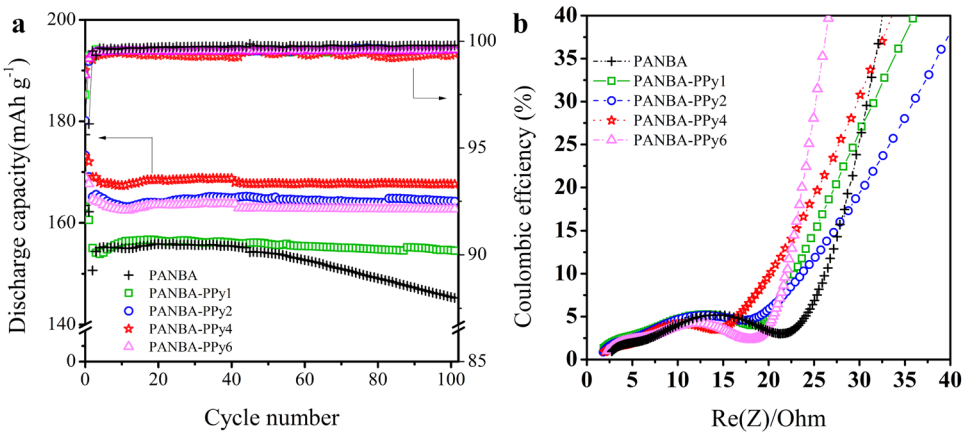

Fig. 5 **a** Cycling performance of the $Li_4Ti_5O_{12}$ electrodes at rates of 0.1C for the first two cycles and 1C for the subsequent 100 cycles. **b** Electrochemical impedance spectra (EIS) of the $Li_4Ti_5O_{12}$ electrodes after charging and discharging at 0.1C for two cycles and 0.5C for a further three cycles.

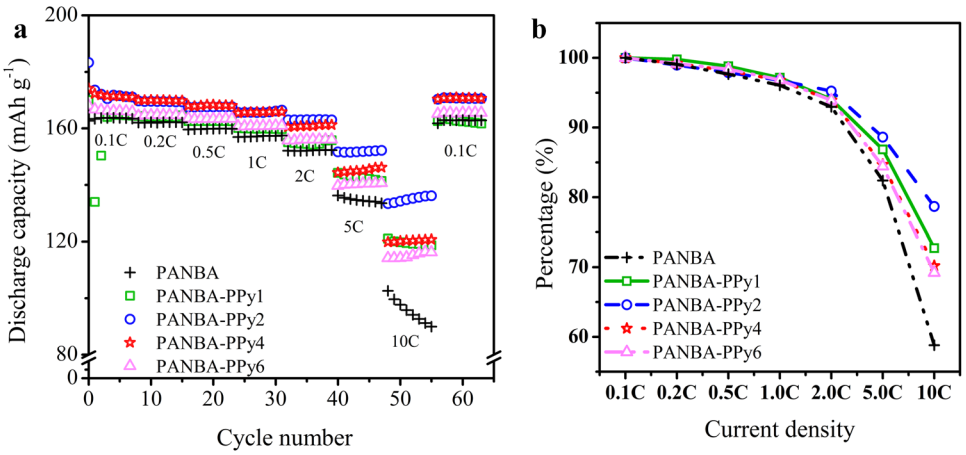

Fig. 6 **a** Cycling behavior of the $Li_4Ti_5O_{12}$ electrodes at rates of 0.1C, 0.2C, 0.5C, 1C, 2C, 5C, and 10C. **b** Percentage of the average capacity at a certain current density compared to the average capacity at 0.1C

materials. At low current rates, the electronic and ionic conductivity should be considered first to achieve good performance, whereas at high current rates, the adhesion capability of the binder should be considered.

4 Conclusion

A conductive PPy component was incorporated successfully into a water-dispersed PANBA binder using a two-step emulsion polymerization process. The conductive PANBA-PPy emulsified binders were applied to LTO electrodes for the first time. The LTO electrodes containing the conductive PANBA-PPy binders showed outstanding rate capability and stable long-life cycling performance. This was attributed to the combination of the adhesive segment of PANBA with the conductive segment PPy in the binder system. Among the LTO electrodes, the LTO electrode containing the PANBA-PPy4 binder, which was copolymerized with 4 g of pyrrole in 30 g of PANBA, had lower charge transfer and electrical resistance and thus better initial discharge capacity, coulombic efficiency, and capacity retention during the charge/discharge process at a 1 C current rate than the other electrodes containing the other conductive PANBA-PPy binders and non-conductive PANBA binder. In contrast, PANBA-PPy2 showed remarkable performance in the high current rate cycling test: discharge capacities of 152 mAh g^{-1} and 136 mAh g^{-1} at 5 C and 10 C, respectively. This is because PANBA-PPy2 has stronger adhesion capability than PANBA-PPy4 that allows it to endure the impact caused by the high current density.

Acknowledgements The study was supported by the 2019 research fund of the University of Ulsan.

Reference

1. Zuo X, Zhu J, Müller-Buschbaum P, Cheng Y-J (2017) Silicon based lithium-ion battery anodes: a chronicle perspective review. Nano Energy 31:113–143. https://doi.org/10.1016/j.nanoen.2016.11.013
2. Manthiram A (2017) An outlook on lithium ion battery technology. ACS Cent Sci 3:1063–1069. https://doi.org/10.1021/acscentsci.7b00288
3. Hu B, Shkrob IA, Zhang S et al (2018) The existence of optimal molecular weight for poly(acrylic acid) binders in silicon/graphite composite anode for lithium-ion batteries. J Power Sources 378:671–676. https://doi.org/10.1016/j.jpowsour.2017.12.068
4. Cao P-F, Naguib M, Du Z et al (2018) Effect of binder architecture on the performance of silicon/graphite composite anodes for lithium ion batteries. ACS Appl Mater Interfaces 10:3470–3478. https://doi.org/10.1021/acsami.7b13205
5. Gendensuren B, Oh E-S (2018) Dual-crosslinked network binder of alginate with polyacrylamide for silicon/graphite anodes of lithium ion battery. J Power Sources 384:379–386. https://doi.org/10.1016/j.jpowsour.2018.03.009
6. Magasinski A, Zdyrko B, Kovalenko I et al (2010) Toward efficient binders for Li-ion battery Si-based anodes: polyacrylic acid. ACS Appl Mater Interfaces 2:3004–3010. https://doi.org/10.1021/am100871y
7. Komaba S, Yabuuchi N, Ozeki T et al (2012) Comparative study of sodium polyacrylate and poly(vinylidene fluoride) as binders for high capacity Si–graphite composite negative electrodes in Li-ion batteries. J Phys Chem C 116:1380–1389. https://doi.org/10.1021/jp204817h
8. Hays KA, Ruther RE, Kukay AJ et al (2018) What makes lithium substituted polyacrylic acid a better binder than polyacrylic acid for silicon-graphite composite anodes? J Power Sources 384:136–144. https://doi.org/10.1016/j.jpowsour.2018.02.085
9. Zhu X, Zhang F, Zhang L et al (2018) A highly stretchable cross-linked polyacrylamide hydrogel as an effective binder for silicon and sulfur electrodes toward durable lithium-ion storage. Adv Funct Mater 28:1705015. https://doi.org/10.1002/adfm.201705015
10. Choi S, Kwon T, Coskun A, Choi JW (2017) Highly elastic binders integrating polyrotaxanes for silicon microparticle anodes in lithium ion batteries. Science 357:279–283. https://doi.org/10.1126/science.aal4373

11. Kovalenko I, Zdyrko B, Magasinski A et al (2011) A major constituent of brown algae for use in high-capacity Li-ion batteries. Science 334:75–79. https://doi.org/10.1126/science.1209150
12. De Giorgio F, La Monaca A, Dinter A et al (2018) Water-processable Li4Ti5O12 electrodes featuring eco-friendly sodium alginate binder. Electrochim Acta 289:112–119. https://doi.org/10.1016/j.electacta.2018.09.017
13. Liu G, Xun S, Vukmirovic N et al (2011) Polymers with tailored electronic structure for high capacity lithium battery electrodes. Adv Mater 23:4679–4683. https://doi.org/10.1002/adma.201102421
14. Han S-W, Kim S-J, Oh E-S (2014) Significant performance enhancement of $Li_4Ti_5O_{12}$ electrodes using a graphene-polyvinylidene fluoride conductive composite binder. J Electrochem Soc 161:A587–A592. https://doi.org/10.1149/2.035404jes
15. Ma X, Zou S, Tang A et al (2018) Three-dimensional hierarchical walnut kernel shape conducting polymer as water soluble binder for lithium-ion battery. Electrochim Acta 269:571–579. https://doi.org/10.1016/j.electacta.2018.03.031
16. Zeng W, Wang L, Peng X et al (2018) Enhanced ion conductivity in conducting polymer binder for high-performance silicon anodes in advanced lithium-ion batteries. Adv Energy Mater 8:1702314. https://doi.org/10.1002/aenm.201702314
17. Zhao H, Wei Y, Wang C et al (2018) Mussel-inspired conductive polymer binder for Si-alloy anode in lithium-ion batteries. ACS Appl Mater Interfaces 10:5440–5446. https://doi.org/10.1021/acsami.7b14645
18. Zhao H, Du A, Ling M et al (2016) Conductive polymer binder for nano-silicon/graphite composite electrode in lithium-ion batteries towards a practical application. Electrochim Acta 209:159–162. https://doi.org/10.1016/j.electacta.2016.05.061
19. Jeschull F, Brandell D, Wohlfahrt-Mehrens M, Memm M (2017) Water-soluble binders for lithium-ion battery graphite electrodes: slurry rheology, coating adhesion, and electrochemical performance. Energy Technol 5:2108–2118. https://doi.org/10.1002/ente.201700200
20. Wang R, Feng L, Yang W et al (2017) Effect of different binders on the electrochemical performance of metal oxide anode for lithium-ion batteries. Nanoscale Res Lett.https://doi.org/10.1186/s11671-017-2348-6
21. Zheng H, Liu G, Song X et al (2010) Optimization of ratio and amount of CMC/SBR binder for a graphite anode. 218th ECS Meeting Abstracts, 200
22. Nguyen MHT, Oh E-S (2013) Application of a new acrylonitrile/butylacrylate water-based binder for negative electrodes of lithium-ion batteries. Electrochem Commun 35:45–48. https://doi.org/10.1016/j.elecom.2013.07.042
23. Nguyen MHT, Oh E-S (2015) Improvement of the characteristics of poly(acrylonitrile–butylacrylate) water-dispersed binder for lithium-ion batteries by the addition of acrylic acid and polystyrene seed. J Electroanal Chem 739:111–114. https://doi.org/10.1016/j.jelechem.2014.12.026
24. Lee K, Kim T-H (2018) Poly(aniline-co-anthranilic acid) as an electrically conductive and mechanically stable binder for high-performance silicon anodes. Electrochim Acta 283:260–268. https://doi.org/10.1016/j.electacta.2018.06.175
25. Luo Y, Guo R, Li T et al (2018) Applications of polyaniline for Li-ion batteries, Li-sulfur batteries and supercapacitors. ChemSusChem. https://doi.org/10.1002/cssc.201802186
26. Gao H, Lu Q, Yao Y et al (2017) Significantly raising the cell performance of lithium sulfur battery via the multifunctional polyaniline binder. Electrochim Acta 232:414–421. https://doi.org/10.1016/j.electacta.2017.02.160
27. Das PR, Gräfenstein A, Ledwoch D et al (2014) Conducting polymers as binder additives for cathodes in Li ion battery. ECS Trans 63:31–43. https://doi.org/10.1149/06301.0031ecst
28. Zhong H, He A, Lu J et al (2016) Carboxymethyl chitosan/conducting polymer as water-soluble composite binder for $LiFePO_4$ cathode in lithium ion batteries. J Power Sources 336:107–114. https://doi.org/10.1016/j.jpowsour.2016.10.041
29. Lee K, Lim S, Tron A et al (2016) Polymeric binder based on PAA and conductive PANI for high performance silicon-based anodes. RSC Adv 6:101622–101625. https://doi.org/10.1039/C6RA23805J
30. Vernitskaya TV, Efimov ON (1997) Polypyrrole: a conducting polymer; its synthesis, properties and applications. Russ Chem Rev 66:443. https://doi.org/10.1070/RC1997v066n05ABEH000261
31. Maruthamuthu S, Chandrasekaran J, Manoharan D, Magesh R (2015) Conductivity and dielectric analysis of Nanocolloidal polypyrrole particles functionalized with higher weight percentage of poly(styrene sulfonate) using the dispersion polymerization method. J Polym Eng 37:1–12. https://doi.org/10.1515/polyeng-2015-0321
32. Fu Y, Su Y-S, Manthiram A (2012) Sulfur-polypyrrole composite cathodes for lithium-sulfur batteries. J Electrochem Soc 159:A1420–A1424. https://doi.org/10.1149/2.027209jes
33. Li C, Tan J, Li H et al (2015) Fast magnetic-field-induced formation of one-dimensional structured chain-like materials via sintering of Fe3O4/poly(styrene-co-n-butyl acrylate-co-acrylic acid) hybrid microspheres. RSC Adv 5:28735–28742. https://doi.org/10.1039/C4RA16809G
34. Wu H, Bremner DH, Li H et al (2016) A novel multifunctional biomedical material based on polyacrylonitrile: preparation and characterization. Mater Sci Eng C 62:702–709. https://doi.org/10.1016/j.msec.2016.02.026
35. Geißler U, Hallensleben ML, Toppare L (1991) Conducting polymer composites of poly(N-methylpyrrole) and poly(bisphenol-A-carbonate). Adv Mater 3:104–106. https://doi.org/10.1002/adma.19910030207
36. Lee B-R, Oh E-S (2013) Effect of molecular weight and degree of substitution of a sodium-carboxymethyl cellulose binder on $Li_4Ti_5O_{12}$ anodic performance. J Phys Chem C 117:4404–4409. https://doi.org/10.1021/jp311678p
37. Chou S-L, Wang J-Z, Liu H-K, Dou S-X (2011) Rapid synthesis of $Li_4Ti_5O_{12}$ microspheres as anode materials and its binder effect for lithium-ion battery. J Phys Chem C 115:16220–16227. https://doi.org/10.1021/jp2039256